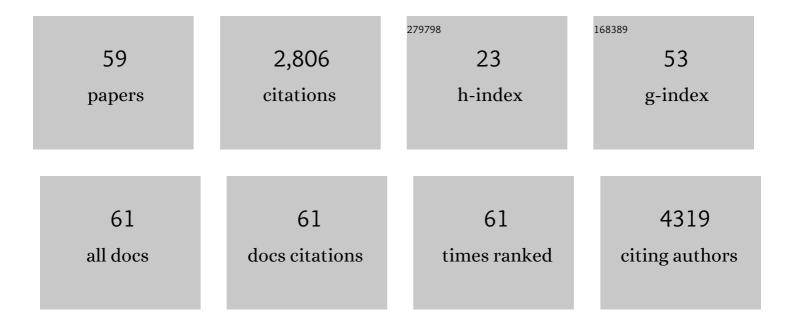
Jaysen Nelayah

List of Publications by Year in descending order

Source: https://exaly.com/author-pdf/1124784/publications.pdf Version: 2024-02-01



INVERN NELAVAH

#	Article	IF	CITATIONS
1	Mapping surface plasmons on a single metallic nanoparticle. Nature Physics, 2007, 3, 348-353.	16.7	908
2	Transition from core–shell to Janus chemical configuration for bimetallic nanoparticles. Nanoscale, 2012, 4, 3381.	5.6	163
3	On the Influence of Oxygen on the Degradation of Feâ€N Catalysts. Angewandte Chemie - International Edition, 2020, 59, 3235-3243.	13.8	160
4	Plasmon Spectroscopy and Imaging of Individual Gold Nanodecahedra: A Combined Optical Microscopy, Cathodoluminescence, and Electron Energy-Loss Spectroscopy Study. Nano Letters, 2012, 12, 4172-4180.	9.1	139
5	On the Influence of Oxygen on the Degradation of Feâ€N Catalysts. Angewandte Chemie, 2020, 132, 3261-3269.	2.0	133
6	Tuning the Performance and the Stability of Porous Hollow PtNi/C Nanostructures for the Oxygen Reduction Reaction. ACS Catalysis, 2015, 5, 5333-5341.	11.2	125
7	Defects do Catalysis: CO Monolayer Oxidation and Oxygen Reduction Reaction on Hollow PtNi/C Nanoparticles. ACS Catalysis, 2016, 6, 4673-4684.	11.2	107
8	Two-Dimensional Quasistatic Stationary Short Range Surface Plasmons in Flat Nanoprisms. Nano Letters, 2010, 10, 902-907.	9.1	103
9	Direct imaging of surface plasmon resonances on single triangular silver nanoprisms at optical wavelength using low-loss EFTEM imaging. Optics Letters, 2009, 34, 1003.	3.3	77
10	Selective hydrogenation of butadiene over TiO ₂ supported copper, gold and gold–copper catalysts prepared by deposition–precipitation. Physical Chemistry Chemical Physics, 2014, 16, 26514-26527.	2.8	67
11	Implementing Structural Disorder as a Promising Direction for Improving the Stability of PtNi/C Nanoparticles. ACS Catalysis, 2017, 7, 3072-3081.	11.2	61
12	Exploring the Formation of Symmetric Gold Nanostars by Liquid-Cell Transmission Electron Microscopy. Nano Letters, 2017, 17, 4194-4201.	9.1	56
13	Electron energy losses in Ag nanoholes—from localized surface plasmon resonances to rings of fire. Optics Letters, 2009, 34, 2150.	3.3	44
14	Au–Rh and Au–Pd nanocatalysts supported on rutile titania nanorods: structure and chemical stability. Physical Chemistry Chemical Physics, 2015, 17, 28112-28120.	2.8	42
15	Performances of an 80–200 kV microscope employing a cold-FEG and an aberration-corrected objective lens. Microscopy (Oxford, England), 2013, 62, 283-293.	1.5	41
16	Nanoalloying bulk-immiscible iridium and palladium inhibits hydride formation and promotes catalytic performances. Nanoscale, 2014, 6, 9955-9959.	5.6	40
17	Atomic-Scale Snapshots of the Formation and Growth of Hollow PtNi/C Nanocatalysts. Nano Letters, 2017, 17, 2447-2453.	9.1	40
18	Hydrogen absorption in 1Ânm Pd clusters confined in MIL-101(Cr). Journal of Materials Chemistry A, 2017, 5, 23043-23052.	10.3	33

JAYSEN NELAYAH

#	Article	IF	CITATIONS
19	Reshaping Dynamics of Gold Nanoparticles under H ₂ and O ₂ at Atmospheric Pressure. ACS Nano, 2019, 13, 2024-2033.	14.6	32
20	Mapping of valence energy losses via energy-filtered annular dark-field scanning transmission electron microscopy. Ultramicroscopy, 2009, 109, 1164-1170.	1.9	28
21	Monitoring the dynamics of cell-derived extracellular vesicles at the nanoscale by liquid-cell transmission electron microscopy. Nanoscale, 2018, 10, 1234-1244.	5.6	28
22	A deep learning approach for determining the chiral indices of carbon nanotubes from high-resolution transmission electron microscopy images. Carbon, 2020, 169, 465-474.	10.3	27
23	Long-range chemical orders in Au–Pd nanoparticles revealed by aberration-corrected electron microscopy. Nanoscale, 2014, 6, 10423-10430.	5.6	25
24	New insights into the mixing of gold and copper in a nanoparticle from a structural study of Au–Cu nanoalloys synthesized via a wet chemistry method and pulsed laser deposition. Physical Chemistry Chemical Physics, 2015, 17, 28339-28346.	2.8	25
25	Nanostructured Nickel Aluminate as a Key Intermediate for the Production of Highly Dispersed and Stable Nickel Nanoparticles Supported within Mesoporous Alumina for Dry Reforming of Methane. Molecules, 2019, 24, 4107.	3.8	25
26	Effect of Atomic Vacancies on the Structure and the Electrocatalytic Activity of Ptâ€rich/C Nanoparticles: A Combined Experimental and Density Functional Theory Study. ChemCatChem, 2017, 9, 2324-2338.	3.7	23
27	Following Ostwald ripening in nanoalloys by high-resolution imaging with single-atom chemical sensitivity. Applied Physics Letters, 2012, 101, 121920.	3.3	22
28	Disentangling the Degradation Pathways of Highly Defective PtNi/C Nanostructures – An Operando Wide and Small Angle X-ray Scattering Study. ACS Catalysis, 2019, 9, 160-167.	11.2	22
29	Ostwald-Driven Phase Separation in Bimetallic Nanoparticle Assemblies. ACS Nano, 2016, 10, 4127-4133.	14.6	19
30	Direct Measurement of the Surface Energy of Bimetallic Nanoparticles: Evidence of Vegard's Rulelike Dependence. Physical Review Letters, 2018, 120, 025901.	7.8	19
31	EFTEM study of surface plasmon resonances in silver nanoholes. Ultramicroscopy, 2010, 110, 1094-1100.	1.9	16
32	Structure–Activity Relationships for the Oxygen Reduction Reaction in Porous Hollow PtNi/C Nanoparticles. ChemElectroChem, 2016, 3, 1591-1600.	3.4	16
33	Quantitative In Situ Visualization of Thermal Effects on the Formation of Gold Nanocrystals in Solution. Advanced Materials, 2021, 33, e2102514.	21.0	15
34	Original Anisotropic Growth Mode of Copper Nanorods by Vapor Phase Deposition. Crystal Growth and Design, 2014, 14, 6350-6356.	3.0	13
35	Selective shortening of gold nanorods: when surface functionalization dictates the reactivity of nanostructures. Nanoscale, 2020, 12, 22658-22667.	5.6	13
36	Revealing Size Dependent Structural Transitions in Supported Gold Nanoparticles in Hydrogen at Atmospheric Pressure. Small, 2021, 17, e2104571.	10.0	13

JAYSEN NELAYAH

#	Article	IF	CITATIONS
37	Driving reversible redox reactions at solid–liquid interfaces with the electron beam of a transmission electron microscope. Journal of Microscopy, 2018, 269, 127-133.	1.8	12
38	Introducing cobalt as a potential plasmonic candidate combining optical and magnetic functionalities within the same nanostructure. Nanoscale, 2021, 13, 2639-2647.	5.6	11
39	Effect of size on the surface energy of noble metal nanoparticles from analytical and numerical approaches. Physical Review B, 2022, 105, .	3.2	10
40	Nanoscale temperature measurement during temperature controlled in situ TEM using Al plasmon nanothermometry. Ultramicroscopy, 2020, 209, 112881.	1.9	9
41	Structural Properties of Catalytically Active Bimetallic Gold–Palladium Nanoparticles Synthesized on Rutile Titania Nanorods by Pulsed Laser Deposition. Crystal Growth and Design, 2018, 18, 68-76.	3.0	8
42	Quantitative insights into the growth mechanisms of nanopores in hexagonal boron nitride. Physical Review Materials, 2020, 4, .	2.4	8
43	Structural analysis of single nanoparticles in liquid by low-dose STEM nanodiffraction. Micron, 2019, 116, 30-35.	2.2	7
44	Thermodynamics of faceted palladium(–gold) nanoparticles supported on rutile titania nanorods studied using transmission electron microscopy. Physical Chemistry Chemical Physics, 2018, 20, 13030-13037.	2.8	3
45	Characterization of the boron profile and coordination in altered glass layers by EEL spectroscopy. Micron, 2021, 141, 102983.	2.2	3
46	Probing surface plasmons on individual nano-objects by near-field electron energy loss spectroscopy. , 2005, , .		2
47	Application of Monochromated Electrons in EELS. Microscopy and Microanalysis, 2008, 14, 134-135.	0.4	2
48	Thickness dependent microstructural changes in La0.5Ca0.5MnO3 thin films deposited on (111) SrTiO3. Thin Solid Films, 2010, 518, 4667-4669.	1.8	2
49	(Invited) Porous Hollow PtNi/C Nanoparticles and Their Many Facets. ECS Transactions, 2017, 80, 731-741.	0.5	2
50	Studying the Effects of Temperature on the Nucleation and Growth of Nanoparticles by Liquid-Cell Transmission Electron Microscopy. Journal of Visualized Experiments, 2021, , .	0.3	2
51	Monitoring Extracellular-Vesicles Dynamics at the Nanoscale by Liquid-Cell TEM. Microscopy and Microanalysis, 2016, 22, 32-33.	0.4	2
52	Low-loss EFTEM Imaging of Surface Plasmon Resonances in Ag Nanostructures. Microscopy and Microanalysis, 2010, 16, 1438-1439.	0.4	1
53	Revealing the Surface Energetics and Reactivity of Bimetallic Copper-Gold Catalyst Nanoparticles by In Situ Environmental TEM. Microscopy and Microanalysis, 2019, 25, 33-34.	0.4	1
54	Revealing the Dynamics of Functional Nanomaterials in Their Formation and Application Media with Liquid and Gas-phase TEM. Microscopy and Microanalysis, 2020, 26, 196-198.	0.4	1

JAYSEN NELAYAH

#	Article	IF	CITATIONS
55	Structural Transformations of Au and Au-Cu Nanoparticles during Liquid-Phase Synthesis and Redox Reactions in Gaseous Environment. Microscopy and Microanalysis, 2017, 23, 1860-1861.	0.4	Ο
56	Probing the Dynamics and the Atomic Structure of Gold Nanorods in Solution with Liquid-Cell TEM. Microscopy and Microanalysis, 2019, 25, 45-46.	0.4	0
57	Corrosion Products Formed on MgZr Alloy Embedded in Geopolymer Used as Conditioning Matrix for Nuclear Waste—A Proposition of Interconnected Processes. Materials, 2021, 14, 2017.	2.9	0
58	Quantitative Study of Temperature Effects on The Nucleation and Growth of Gold Nanocrystals in Water. Microscopy and Microanalysis, 2021, 27, 29-30.	0.4	0
59	Insights into the Structure-Reactivity of Supported Au Nanocatalyst during Butadiene Selective Hydrogenation by Atomic Scale In Situ Environmental TEM. Microscopy and Microanalysis, 2021, 27, 41-42.	0.4	0